

OPEN ACCESS

Projected regime shift in Arctic cloud and water vapor feedbacks

To cite this article: Yonghua Chen *et al* 2011 *Environ. Res. Lett.* **6** 044007

View the [article online](#) for updates and enhancements.

You may also like

- [Effect of focused nanosecond laser pulse irradiation on microtribological properties of diamond-like films](#)
V.D. Frolov, P.A. Pivovarov, E.V. Zavedeev et al.
- [Relation between micro- and nanostructure features and biological properties of the decellularized rat liver](#)
Maria M Bobrova, Liubov A Safonova, Anton E Efimov et al.
- [Two-Dimensional Approximate Analytical Solutions for the Direct Liquid Fuel Cell](#)
Sher Lin Ee and Erik Birgersson

Breath Biopsy Conference

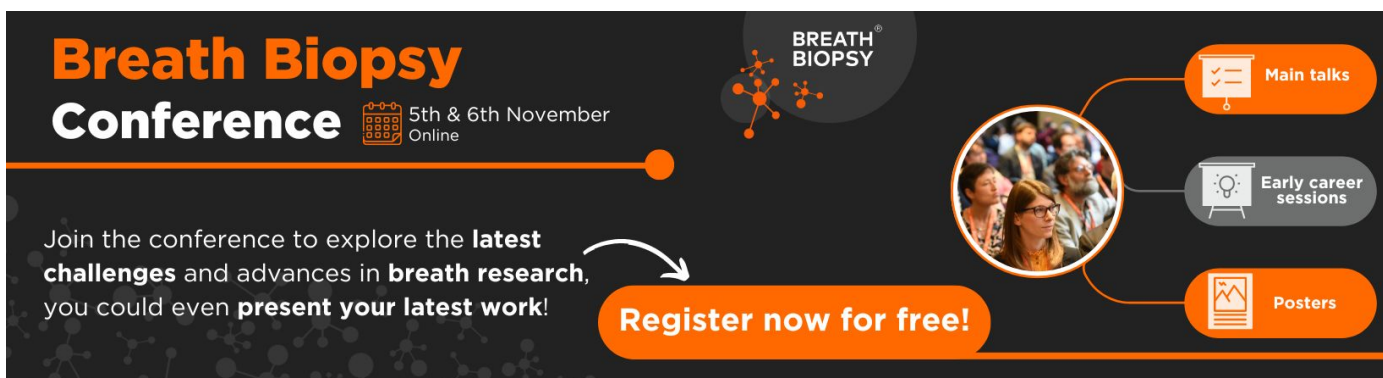
5th & 6th November Online

Join the conference to explore the **latest challenges** and advances in **breath research**, you could even **present your latest work!**

Register now for free!

BREATH BIOPSY

- Main talks
- Early career sessions
- Posters



Projected regime shift in Arctic cloud and water vapor feedbacks

Yonghua Chen¹, James R Miller², Jennifer A Francis²
and Gary L Russell³

¹ Columbia University and Institute for Space Studies, USA

² Department of Marine and Coastal Sciences, Rutgers University, 71 Dudley Road,
New Brunswick, NJ 08901, USA

³ NASA Goddard Institute for Space Studies, 2880 Broadway, New York, NY 10025, USA

E-mail: yc2268@columbia.edu

Received 23 July 2011

Accepted for publication 3 October 2011

Published 25 October 2011

Online at stacks.iop.org/ERL/6/044007

Abstract

The Arctic climate is changing faster than any other large-scale region on Earth. A variety of positive feedback mechanisms are responsible for the amplification, most of which are linked with changes in snow and ice cover, surface temperature (T_s), atmospheric water vapor (WV), and cloud properties. As greenhouse gases continue to accumulate in the atmosphere, air temperature and water vapor content also increase, leading to a warmer surface and ice loss, which further enhance evaporation and WV. Many details of these interrelated feedbacks are poorly understood, yet are essential for understanding the pace and regional variations in future Arctic change. We use a global climate model (Goddard Institute for Space Studies, Atmosphere–Ocean Model) to examine several components of these feedbacks, how they vary by season, and how they are projected to change through the 21st century. One positive feedback begins with an increase in T_s that produces an increase in WV, which in turn increases the downward longwave flux (DLF) and T_s , leading to further evaporation. Another associates the expected increases in cloud cover and optical thickness with increasing DLF and T_s . We examine the sensitivities between DLF and other climate variables in these feedbacks and find that they are strongest in the non-summer seasons, leading to the largest amplification in T_s during these months. Later in the 21st century, however, DLF becomes less sensitive to changes in WV and cloud optical thickness, as they cause the atmosphere to emit longwave radiation more nearly as a black body. This regime shift in sensitivity implies that the amplified pace of Arctic change relative to the northern hemisphere could relax in the future.

Keywords: Arctic, feedback, sensitivity, clouds, water vapor, radiation

1. Introduction

During recent decades, the observed warming in the Arctic region has been substantially larger than that at lower latitudes (e.g., Serreze and Francis 2006). Other Arctic climate variables—such as sea ice extent and volume, precipitable water vapor, permafrost coverage, vegetation, and snow cover—have also changed significantly during the past few decades (e.g., Dickson 1999, Serreze *et al* 2000, Serreze *et al* 2007, Wang and Key 2005). These changes are

occurring on time scales associated with the natural variability related to large-scale patterns such as the North Atlantic/Arctic oscillations and on longer time scales related to increasing levels of atmospheric greenhouse gases (GHGs) (Overland and Wang 2005). Arctic sea ice cover and sea ice thickness have decreased rapidly since 1980 (Cavalieri *et al* 2003, Comiso 2006, Stroeve *et al* 2005, Rothrock *et al* 1999), and the Arctic melt season has lengthened (Markus *et al* 2009, Belchansky *et al* 2004). Francis and Hunter (2006) examined linkages between declining perennial sea ice and atmospheric forcing

variables and found that anomalies in downward longwave radiation were the most important factor driving ice extent variability until 2005.

Several positive feedbacks are involved in exchanges of energy and water mass between the ocean, sea ice, and atmosphere, and contribute to the amplification of high-latitude climate change. The sea ice albedo feedback is among the most important, although there are other less understood but possibly as important feedbacks that result from changes in cloud cover, cloud optical thickness, cloud height, and atmospheric water vapor. Feedbacks related to surface air temperature (T_s) involve a set of climate variables such that a temperature-induced change in one variable causes changes in other variables that ultimately induce a change in the initial temperature perturbation. Chen *et al* (2003, 2006) demonstrated the importance of correctly representing these relationships in global climate models for the Arctic region.

The goal of this study is to identify and quantify relationships among several climate variables in these positive feedback loops within a global climate model. Of particular interest is the sensitivity of downward longwave flux (DLF) to changes in atmospheric water vapor (WV), total cloud cover (CLDT), and cloud optical thickness (COT). This work extends the study of Miller *et al* (2007), who performed a similar analysis for winter, and those results are shown again here for comparison with the other seasons. We examine the seasonal dependences of these relationships as well as how they might change throughout the 21st century as atmospheric greenhouse gases increase. In this study, we focus on the Beaufort Sea area, north of Alaska, as a region representative of central-Arctic conditions characterized by a relatively homogeneous ice pack and atmospheric characteristics. Section 2 provides a brief description of the climate model, the long-term seasonal changes are given in section 3, temporal changes in sensitivities between climate variables are shown in section 4, and a discussion and conclusions are presented in section 5.

2. Model and experiment

The global climate model used in this study is based on, but modified from, Russell *et al* (1995). Simulations from this model have been used in the Intergovernmental Panel on Climate Change (IPCC) Fourth Assessment Report (2007). Both the atmosphere and ocean use the C-grid numerical scheme of Arakawa and Lamb (1977) to solve the momentum equations. The model resolution is $3^\circ \times 4^\circ$ in latitude and longitude with 12 vertical layers in the atmosphere and up to 16 in the ocean. The atmosphere and ocean are coupled synchronously every hour. The atmospheric model uses Russell and Lerner's (1981) linear upstream scheme to advect potential enthalpy and water vapor. All significant atmospheric gases and aerosols are used to calculate the source term. The ocean model has a free surface, employs the linear upstream scheme for the advection of heat and salt, and uses the K-profile parameterization (KPP) of Large *et al* (1994) for the vertical mixing. The model also calculates at each time step the flow of mass, potential enthalpy, and salt through 16 narrow (sub-grid scale) straits in response to the oceanic pressure

gradient between the grid cells on either end of the strait. Freshwater is added directly to the ocean by precipitation and river flow and is removed by evaporation. There is a four-layer thermodynamic sea ice model, and sea ice advection is based on the scheme described in Miller and Russell (1997). River discharge is calculated directly as part of the model simulation according to the river routing scheme of Miller *et al* (1994). Our study region in the Beaufort Sea is centered on the grid cell around 77°N latitude and 156°N longitude.

Two model simulations were integrated from 1850 to 2100. The control simulation assumes the same 1850 atmospheric composition for all years. For the anthropogenic climate change (ACC) experiment, the observed concentrations of greenhouse gases and estimates of tropospheric sulfate aerosols are updated continuously from 1850 to 2003, followed by projections of greenhouse gases and aerosols from 2004 to 2100 based on the IPCC Special Report on Emissions Scenarios (SRES) A1B scenario (IPCC 2007). SRES A1B is considered a moderately increasing greenhouse gas scenario. It is based on assumptions about future rates of economic and population growth and the development and incorporation of new technologies that increase energy efficiency. The changes in tropospheric sulfate aerosols through 2100 are based on Pham *et al* (2005).

3. Long-term seasonal changes

In this section we examine how surface temperature (T_s), total-column atmospheric water vapor (WV), total cloud cover (CLDT), cloud optical thickness (COT), and downwelling longwave flux (DLF) vary seasonally through the 21st century as global concentrations of greenhouse gases continue to increase in the Beaufort Sea region. The model trends are compared with values from the 40 year European Centre for Medium-Range Weather Forecasts (ECMWF) reanalysis (ERA-40, Uppala *et al* 2005) during the latter part of the 20th century. Figures 1 through 4 show the seasonal variations beginning with the onset of the cooling season in autumn and progressing through winter, spring, and summer. Total changes for different quantities are determined from differences of 20 year averages; trends and changes per decade are based on least square linear fits. The comparison between the model output and ERA-40 reanalysis is for the period of 1960–2000. Table 1 contains total projected changes between two 20 year intervals at the beginning and end of the 150 year period, as well as the mean value for the late 20th century.

Figure 1(a) shows that the autumn (September, October, November) T_s in the ACC experiment increases through the 21st century, with a total increase of 6.1°C . Between 1960 and 2000 the model's temperature increases at a rate of $0.65^\circ\text{C}/\text{decade}$, which is twice that of the ERA-40 trend of $0.30^\circ\text{C}/\text{decade}$. Figure 1(b) shows that there is also a positive trend in DLF during the 150 year simulation, with a total increase of about 30 W m^{-2} or 12%. Evidence supporting the role of changes in WV and cloud properties in contributing to the positive feedback on T_s through DLF is provided by figures 1(c)–(e), which show that WV increases by 35%, CLDT by 20% and COT by 42% (table 1).

Table 1. Mean values of surface air temperature (T_s), downward longwave flux (DLF), atmospheric water vapor (WV), total cloud cover (CLDT), and cloud optical thickness (COT) for the first 20 year period, and the projected changes between two 20 year intervals at the beginning and end of the 150 year period. The percentage change in a variable is shown in parentheses and is with respect to the 20 year period of 1961–80.

	1961–80 (Mean values)				(2081–2100) minus (1961–80) (% changes)			
	SON	DJF	MAM	JJA	SON	DJF	MAM	JJA
T_s ($^{\circ}\text{C}$)	-11.6	-24.3	-15.5	-0.64	6.1	6.2	4.7	0.4
DLF (W m^{-2})	237.8	182.6	215.6	293.4	30 (12)	26.2 (14)	24 (11)	6 (2)
WV (kg m^{-2})	5.25	2.51	3.81	11.51	1.83 (35)	0.80 (32)	1.59 (42)	2.93 (25)
CLDT (%)	69.8	39.6	55.4	88.4	14 (20)	14 (35)	10.7 (19)	0.5 (1)
COT	9.24	4.12	4.75	14.17	3.84 (42)	1.61 (39)	2.52 (53)	3.07 (22)

Figure 2(a) shows that the T_s in winter increases steadily for the first half of the 21st century in the ACC experiment, after which the warming discontinues. The total increase in T_s is 6.2°C . Between 1960 and 2000 the model’s temperature increases at a rate of $0.55^{\circ}\text{C}/\text{decade}$, while the ERA-40 reanalysis shows no trend during this period. As in autumn, figure 2(b) shows that the model projects an increasing trend in DLF at the surface, which is again consistent with concurrent increases in WV, CLDT, and COT (figures 2(c)–(e)), suggesting a positive feedback on T_s . In these figures, the increases in climate variables are most rapid during the first half of the 21st century, while once again the rate of change in the second half is substantially smaller. Other studies describe enhanced wintertime warming during recent decades and suggest that a response to increased water vapor and cloud cover likely played a role (Chen *et al* 2006, Miller and Russell 2002, Wang and Key 2005).

The corresponding set of plots for spring (figure 3) also shows that T_s in the ACC experiment increases through the 21st century by 4.7°C . Between 1960 and 2000 the modeled rate of warming is $0.52^{\circ}\text{C}/\text{decade}$, which is again higher than the ERA-40 warming trend of $0.32^{\circ}\text{C}/\text{decade}$. Figure 3(b) shows that there is also an increasing trend in DLF during the 150 year simulation, with a total increase of 24 W m^{-2} or about 11% (table 1). Figures 3(c)–(e) illustrate WV increasing by 42%, CLDT by 19% (table 1) and COT by 53% (table 1), which are again consistent with the increase in DLF. Starting in the mid-21st century, the positive trends decrease in all variables except WV.

Summer exhibits a different behavior compared with the other three seasons. The major differences arise because the ice surface temperature is nearly constant at the melting point and because the surface energy balance is dominated by insolation rather than longwave radiation. Figure 4(a) shows that the summer T_s in the ACC experiment increases by only 0.38°C through the 21st century. Between 1960 and 2000 the model’s increase of $0.04^{\circ}\text{C}/\text{decade}$ is consistent with ERA-40’s warming of $0.05^{\circ}\text{C}/\text{decade}$. Figure 4(b) shows an increasing trend in DLF during the 150 year simulation, with a total increase of about 6 W m^{-2} or 2% (table 1). Because WV, CLDT and COT are already high in summer, the DLF is not as sensitive to changes in these variables as during the

cold seasons when their mean magnitudes are relatively small. Figures 4(c)–(e) show that WV increases by 25% (table 1), which follows increasing upper air temperatures (not shown) and the resulting increase in saturation vapor pressure. There is little change in CLDT, and a relatively small change in COT compared to other seasons. In fact, cloud cover only increases by 1% (table 1), while both water vapor and cloud optical thickness increase by about 20% (table 1).

Figures 1 through 4 illustrate both observed and projected changes in climate variables in the 20th and 21st centuries, with clear reductions in the pace of change toward the end of the 21st century. This behavior implies that the Arctic will respond differently in decades to come, as ice and snow cover are dramatically reduced from their relatively stable states of the 20th century. There are several possible explanations for the changes simulated by the model. One is that the A1B scenario’s greenhouse forcing decreases later in the 21st century. Even though most greenhouse gases do decrease by mid-21st century in this scenario, WV continues to increase in response to the long residence time of greenhouse gases in the atmosphere. Another explanation is that temporal changes occur in the relationships between variables, which in turn lead to changes in the strengths of the feedbacks. For example, a positive feedback on T_s results from the increase in DLF that occurs in response to increasing levels of WV as the climate warms. In section 4 we examine temporal changes in the sensitivity of DLF to WV, CLDT, and COT. Although we do not specifically address potential changes in downward incident shortwave radiation flux (DSF) in our analysis, we found that during autumn and winter, DSF decreases in response to increased CLDT and COT, but the change is only 15% as large as the change in DLF. In summer, the increase in COT dominates and leads to a net decrease in the DSF (not shown), which is 9 W m^{-2} larger than the increase in DLF.

4. Temporal changes in sensitivities between climate variables

Table 2 lists the seasonal variability in sensitivities between DLF and other variables. All the sensitivities are significant at the 95% level, and the confidence interval bands of the

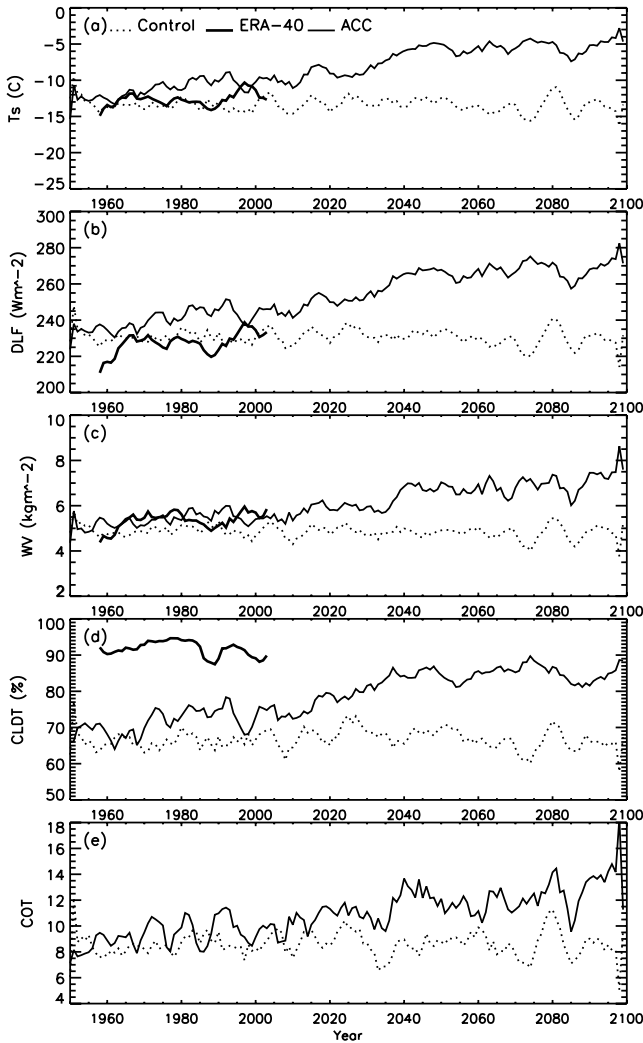


Figure 1. Climate variables during autumn for the control simulation (dotted) and the ACC (anthropogenic climate change) experiment (solid) from 1950 to 2100 in the Beaufort Sea region (approximately 74°N–81°N and 190°E–220°E) for (a) surface air temperature (T_s , °C), (b) downward longwave flux (DLF, W m^{-2}), (c) atmospheric water vapor (WV, kg m^{-2}), (d) total cloud cover (CLDT, %), and (e) cloud optical thickness (COT). The ERA-40 observations (thick solid) for T_s , DLF, and WV are shown for the period from 1960 to 2000.

sensitivities for the 1961–80 period do not overlap with those for the period of 2046–65 when the largest changes in sensitivities occur. This indicates that the changes in sensitivities between these two periods are significant at the 95% level. As Chen *et al* (2006) found, the relationship between DLF and WV varies with water vapor content. One of the factors that makes the water vapor feedback so strong during the Arctic winter in the early years of the model simulation is that the mean concentration of WV is low (2.2 kg m^{-2} , see figure 1). Between 1961 and 1980, DLF in the ACC experiment increases by 19.8 W m^{-2} in winter for every one kg m^{-2} increase in water vapor. However, by the middle of the 21st century, DLF increases by only 13.3 W kg^{-1} because DLF becomes less sensitive to changes in WV as moisture content increases and the emissivity of the

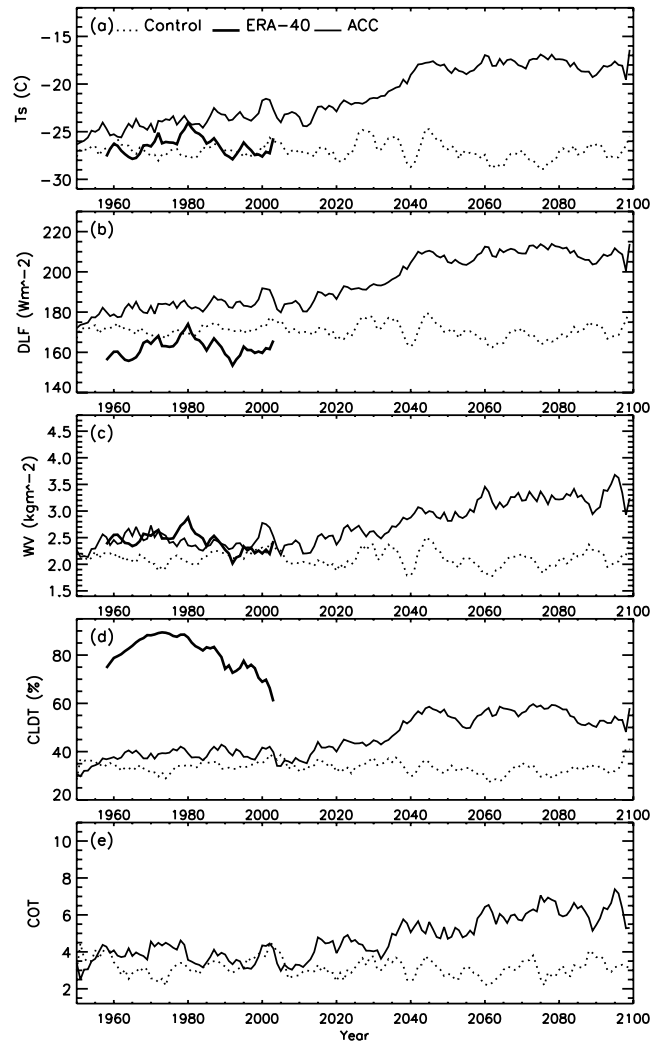


Figure 2. Same as figure 1 but for winter. Modified after Miller *et al* (2007).

atmosphere approaches unity in water vapor’s emission bands. The same behavior is evident for COT. This reduction in the sensitivity of DLF to WV and COT by about a third is at least partly responsible for the slower rate of temperature change during winter toward the end of the 21st century.

Table 2 also presents the temporal changes in the sensitivities of DLF to CLDT and COT during spring, summer, and autumn. There are no significant changes in the sensitivity of DLF to CLDT for any season except winter, when there is a 10% decrease during the century. Significant decreases in the sensitivity of DLF to COT are evident in all seasons, however, ranging from a 50% reduction in autumn to a 25% reduction in summer. In winter the reduction in DLF in response to changes in cloud optical thickness (40%) is slightly larger than the reduction in the sensitivity of DLF to WV.

To examine the seasonal and long-term changes in sensitivities in more detail, we next examine the monthly changes in sensitivities for each of the 20 year periods presented in table 2. The monthly sensitivities are significant at the 95% level. For non-summer months, the changes in sensitivity from 1961–80 to 2046–65 are also significant at the

Table 2. Sensitivity of modeled downward longwave flux (DLF) at the surface to three other climate variables: atmospheric water vapor, cloud cover, and cloud optical thickness. The sensitivities are obtained by generating a scatter plot of the daily average differences of DLF between two consecutive days versus the daily differences of each of the other three variables separately and then calculating the slope of the best-fit line. The four numbers in a cell represent sensitivities for autumn (SON), winter (DJF), spring (MAM), and summer (JJA), respectively. These relationships for the SHEBA region in the Arctic Ocean are obtained from the transient experiment for the three different 20 year periods shown. The winter numbers are the same as those shown in Miller *et al* (2007).

	1961–80				2046–65				2081–2100			
	SON	DJF	MAM	JJA	SON	DJF	MAM	JJA	SON	DJF	MAM	JJA
DLF versus water vapor ($W\text{ kg}^{-1}$)	10.5	19.8	15.7	4.2	6.8	13.3	10.4	3.2	5.6	12.4	10.6	2.9
DLF versus cloud cover ($W\text{ m}^{-2}\ \%^{-1}$)	0.84	0.82	0.80	0.73	0.82	0.74	0.77	0.72	0.84	0.74	0.77	0.69
DLF versus cloud optical thickness ($W\text{ m}^{-2}$)	1.60	3.80	3.0	0.7	0.9	2.2	1.7	0.5	0.8	2.0	1.9	0.5

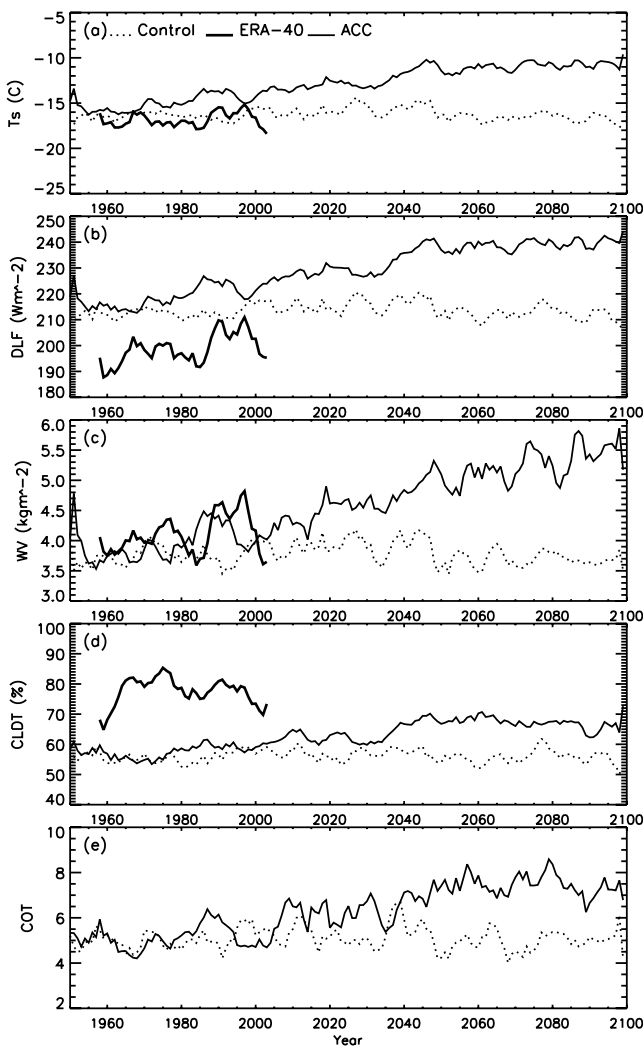


Figure 3. Same as figure 1 but for spring.

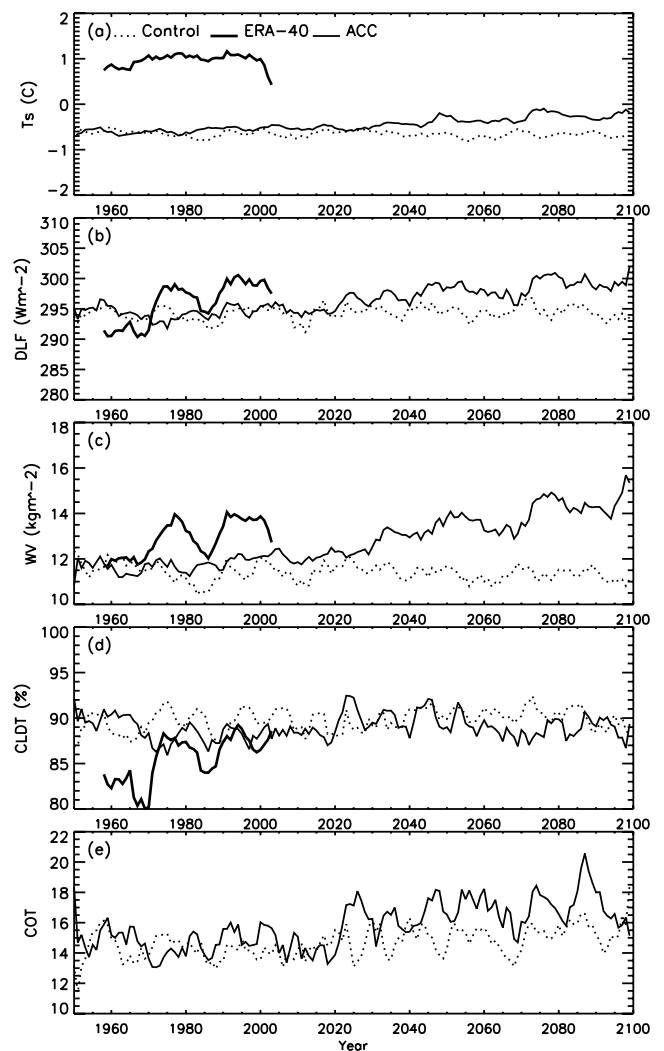


Figure 4. Same as figure 1 but for summer.

95% level. Figures 5 and 6 show the annual cycle of sensitivity of DLF to WV and COT for the three 20 year periods. During all the time intervals, the sensitivities are highest in winter and lowest in summer because the average values of WV and COT are relatively low in winter and high in summer. As

discussed above, when the background values of WV and COT are low, the sensitivity of DLF to changes in these variables is high. Conversely, when the background values are high, as in summer, the DLF response is nearly saturated so that additional changes in WV or COT cause almost no change

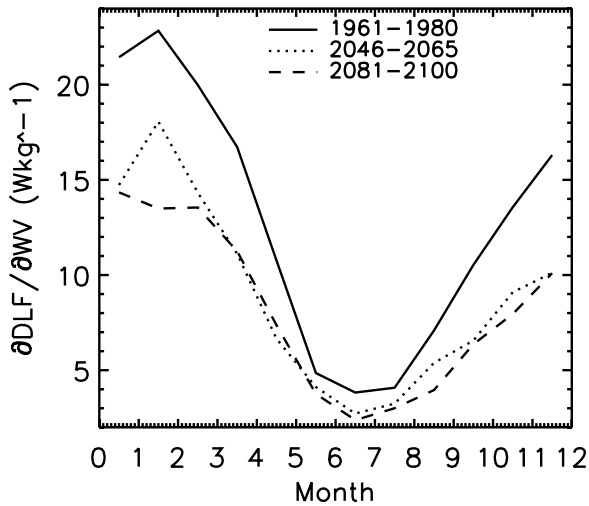


Figure 5. Annual cycle of sensitivity of modeled downward longwave flux (DLF) at the surface to atmospheric water vapor (WV) for three 20 year periods (1961–80, 2046–55, 2081–2100). Monthly sensitivities are obtained by generating a scatter plot of the daily average differences of DLF between two consecutive days versus the daily differences in WV for the same two days and then calculating the slope of the best-fit line.

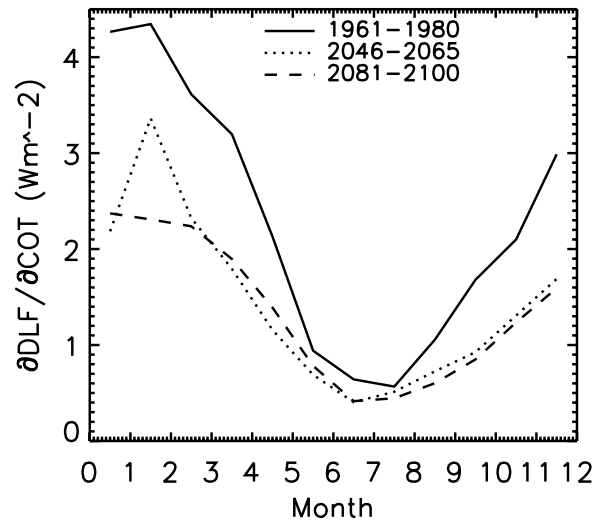


Figure 6. Same as figure 5 but for DLF versus cloud optical thickness (COT).

in DLF. Figures 5 and 6 also show that the largest long-term changes in sensitivity occur in winter while the smallest changes occur in summer. The sensitivity is largest in the 20th century and decreases in all months during the 21st century, with the largest changes during winter. This implies that the strengths of these components of the feedback loops weaken during the 21st century.

Figure 7 shows the annual cycle of sensitivity of DLF to CLDT for the three 20 year periods. Of the three variables, the sensitivity of DLF to CLDT has the weakest seasonal variation, although it is about 15% less than the annual mean in June and July and 10% higher in September. The changes from the 20th to 21st century are small in half the months—of the order of 10% lower in January, February, June, August, and September. July is anomalous as the sensitivity has increased by about 10% during the 21st century. These relatively small changes in sensitivities imply that as the cloud fraction exceeds approximately 50%, any further addition of cloud cover has relatively little effect on DLF. Thus if cloud cover continues to increase in the future as projected by this model, the cloud cover feedback on T_s could become less important as a contributor to Arctic amplification. Because the simulation of clouds accounts for large uncertainties among climate models, this reduced sensitivity may reduce discrepancies among model simulations of Arctic change.

5. Discussion and conclusions

The focus of this letter is on feedbacks in the Arctic climate system with an emphasis on both seasonal and long-term variability in the sensitivity of DLF to changes in WV and cloud properties in a global climate model. Seasonally, the sensitivity of DLF to changes in WV or COT is largest

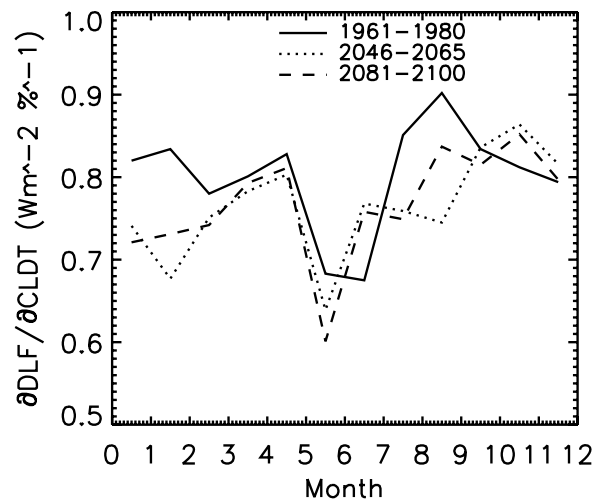


Figure 7. Same as figure 5 but for DLF versus cloud cover (CLDT).

in winter, somewhat smaller in the transition seasons, and smallest in summer. There is much less seasonal variability in the sensitivity of DLF to CLDT. By the mid- to late-21st century, the sensitivity of DLF to changes in WV or COT is projected to decrease substantially in autumn, winter, and spring, with the largest changes in winter. The changes in summer are small. However, the sensitivity of DLF to changes in cloud cover is somewhat smaller during the 21st century than it is today, especially in winter.

These results are consistent with previous studies (Miller *et al* 2007, Francis and Hunter 2007, Miller and Russell 2002) that identified increasing DLF—owing primarily to increasing WV, CLDT, and COT—as playing an important role in the present-day Arctic system. Our findings are also consistent with other studies suggesting that the strengths of these relationships may depend on the mean values of each climate variable during a specific period of time (Chen *et al* 2006). The sensitivity of DLF to long-term changes in WV

and COT in winter, autumn and spring decreases in response to what can be characterized as a regime shift in atmospheric emission: from a low range toward the end of the 20th century to a higher range near the middle of the 21st century. In other words, the sensitivity of DLF and T_s to changes in water vapor (cloud optical thickness) is larger in a drier atmosphere. The regime shift in atmospheric emissivity is responsible for a corresponding regime shift in the positive feedback on T_s because additional increases in WV that are induced by increases in air temperature cause smaller increases in DLF than in the earlier regime with less WV. Hence, the positive feedback on T_s weakens. The same regime shift occurs with increasing COT, likely owing to an increase in liquid-containing clouds as the Arctic warms, leading to an atmospheric emissivity approaching unity.

As a check on the model's ability to represent sensitivities, we compare the model's sensitivities for spring with those obtained by Francis and Hunter (2007) using satellite retrievals in the Beaufort Sea. For the last two decades of the 20th century, their sensitivity of DLF to changes in WV during spring was 14.6 W kg^{-1} , which is similar to the model's sensitivity of 15.7 W kg^{-1} for 1961–80. Their sensitivity of DLF to CLDT was 0.74 W m^{-2} compared to the model's value of 0.80 W m^{-2} . We also compared the model's monthly sensitivity of DLF to changes in WV for the 1961–80 period with the corresponding ERA-40 daily values for the Beaufort region, and found the same strong seasonal signal, although the model's sensitivity was lower in all months, by 15% in February, which is the month of peak sensitivity, and somewhat more in late autumn. As a further check on our results, we calculated the same sensitivities as above but for the entire Arctic Ocean and found that the sensitivities were similar to those in table 2. For the entire Arctic, the conclusions derived from our analysis of the Beaufort Sea region regarding both seasonal and long-term changes in the sensitivities are consistent with our results here.

The focus of this letter has been on the sensitivity of DLF to three climate variables in the model: atmospheric water vapor, cloud cover, and cloud optical thickness. The total future change in DLF with respect to any of these variables will depend on two factors—one is the sensitivity, as discussed in this letter, and the other is the total change in each of the climate variables. For example, the total change in DLF in response to WV for a multi-decadal period would be the time-integrated product of the sensitivity of DLF to WV and the change in WV during the period. Table 1 shows the percentage change in each of the climate variables during the 21st century and, along with table 2, provides evidence of the relative roles of sensitivity and net changes in the value of a specific variable in contributing to the total change in DLF. For climate models to predict future climate change, they must be able to not only represent the sensitivities between climate variables, as discussed here, but they must also be able to correctly predict the net changes in the corresponding climate variables. The accuracy of any model's projections, therefore, depends on future emissions of greenhouse gases and other human-caused as well as natural changes to the Earth's atmosphere and surface.

Acknowledgments

We would like to acknowledge support for this study from NASA grant NAG5-11720. Partial support for James R Miller was provided by Project #32103 of the New Jersey Agricultural Experiment Station, and for J Francis from NSF/ARCSS grant 0628818. The ERA-40 reanalysis data were obtained from the ECWMF data server. We are also grateful to Elias Hunter for providing some of the ERA-40 data. The authors thank two reviewers for their comments that improved this study.

References

- Arakawa A and Lamb V R 1977 Computational design of the basic dynamical processes of the UCLA general circulation model *Methods Comput. Phys.* **17** 337
- Belchansky G I, Douglas D C and Platonov N G 2004 Duration of the Arctic sea ice melt season: regional and interannual variability 1979–2001 *J. Clim.* **17** 67–80
- Cavalieri D J, Parkinson C L and Vinnikov K Y 2003 30-Year satellite record reveals contrasting Arctic and Antarctic decadal sea ice variability *Geophys. Res. Lett.* **30** 41–4
- Chen Y, Aires F, Francis J A and Miller J R 2006 Observed relationships between Arctic longwave cloud forcing and cloud parameters using a neural network *J. Clim.* **19** 4087–104
- Chen Y, Miller J R, Francis J A, Russell G L and Aires F 2003 Observed and modeled relationships among Arctic climate variables *J. Geophys. Res.* **108** 4799
- Comiso J C 2006 Arctic warming signals from satellite observations *Weather* **61** 70–6
- Dickson B 1999 All change in the Arctic *Nature* **397** 389–91
- Francis J A and Hunter E 2006 New insight into the disappearing Arctic sea ice *Eos Trans.* **87** 509–24
- Francis J A and Hunter E 2007 Changes in the fabric of the Arctic's greenhouse blanket *Environ. Res. Lett.* **2** 045001
- IPCC (Intergovernmental Panel on Climate Change) 2007 *Climate Change 2007: The Physical Science Basis. Contribution of Working Group I to the Fourth Assessment Report of the Intergovernmental Panel on Climate Change* ed S Solomon, D Qin, M Manning, Z Chen, M Marquis, K B Averyt, M Tignor and H L Miller (Cambridge: Cambridge University Press)
- Large W G, McWilliams J C and Doney S C 1994 Oceanic vertical mixing: review and a model with non-local boundary layer parameterization *Rev. Geophys.* **32** 363–403
- Markus T, Stroeve J C and Miller J 2009 Recent changes in Arctic sea ice melt onset, freezeup, and melt season length *J. Geophys. Res.* **114** C12024
- Miller J R, Chen Y, Russell G L and Francis J A 2007 Future regime shift in feedbacks during Arctic winter *Geophys. Res. Lett.* **34** L23707
- Miller J R and Russell G L 1997 Investigating the interactions among river flow, salinity, and sea ice using a global coupled atmosphere-ocean-ice model *Ann. Glaciol.* **25** 121–6
- Miller J R and Russell G L 2002 Projected impact of climate change on the energy budget of the Arctic Ocean by a global climate model *J. Clim.* **15** 3028–42
- Miller J R, Russell G L and Caliri G 1994 Continental scale river flow in climate models *J. Clim.* **7** 914–28
- Overland J E and Wang M 2005 The Arctic climate paradox: the recent decrease of the Arctic oscillation *Geophys. Res. Lett.* **32** L06701
- Pham M, Boucher O and Hauglustaine D 2005 Changes in atmospheric sulfur burdens and concentrations and resulting radiative forcings under the IPCC SRES emission scenarios for 1990–2100 *J. Geophys. Res.* **110** D06112

- Rothrock D A, Yu Y and Maykut G A 1999 Thinning of the Arctic sea-ice cover *Geophys. Res. Lett.* **26** 3469–72
- Russell G L and Lerner J A 1981 A new finite differencing scheme for the tracer transport equation *J. Appl. Meteorol.* **20** 1483–98
- Russell G L, Miller J R and Rind D 1995 A coupled atmosphere-ocean model for transient climate change studies *Atmos.-Ocean* **33** 683–730
- Serreze M C and Francis J A 2006 The Arctic amplification debate *Clim. Change* **76** 241–64
- Serreze M C, Holland M M and Stroeve J 2007 Perspectives on the Arctic's shrinking sea-ice cover *Science* **315** 1553–6
- Serreze M C, Walsh J E, Chapin F S III, Osterkamp T, Dyurgerov M, Romanovsky V, Oechel W C, Morison J, Zhang T and Barry R G 2000 Observational evidence of recent change in the northern high-latitude environment *Clim. Change* **46** 159–207
- Stroeve J C, Serreze M C, Fetterer F, Arbetter T, Meier W, Maslanik J and Knowles K 2005 Tracking the Arctic's shrinking ice cover: another extreme September minimum in 2004 *Geophys. Res. Lett.* **32** L04501
- Uppala S M *et al* 2005 The ERA-40 re-analysis *Quart. J. R. Meteorol. Soc.* **131** 2961–3012
- Wang X and Key J R 2005 Arctic surface, cloud, and radiation properties based on the AVHRR polar pathfinder dataset. Part II: recent trends *J. Clim.* **18** 2575–93